

First Principles Investigation of Transition Metal Doped WSe₂ Monolayer for Photocatalytic Water Splitting

Celine Wu and Xuan Luo

National Graphene Research and Development Center, Springfield, Virginia 22151, USA

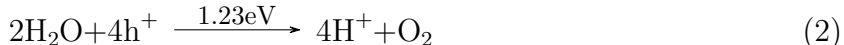
(Dated: January 4, 2022)

arXiv:2201.00396v1 [cond-mat.mtrl-sci] 2 Jan 2022

I. INTRODUCTION

Fossil fuels have been the primary source of energy for the past two centuries¹. However, the growing concern about the use of fossil fuels has drastically increased as its consumption has exceedingly outpaced the amount of resources. In 2018, the United States' energy consumption hit a record high of 101.3 quadrillion British thermal units(Btu)², among which, 80% were fossil fuels^{3,4}. It is predicted that oil will be exhausted in 30 years, gas in 40 years, and coal in 70 years⁵. Consequently, there is a pressing need for renewable energy sources. Recently, photocatalysis, in particular, photocatalytic water splitting, has drawn great attention as an environmentally friendly solution to this crisis by converting solar energy into hydrogen fuel^{6,7}.

Photocatalysis results in the rate change of chemical transformation due to the presence of a photocatalyst, a material which absorbs light and acts as a reagent, but is not consumed in the process^{8,9}. The key to photocatalytic water splitting is the material for the photocatalyst because it absorbs photon energy, which excites electrons from the occupied valence band to the unoccupied conduction band¹⁰. This process generates electron-hole pairs which spread to the surface and take part in the two half-redox reactions. The reactions split the hydrogen-oxygen bond [$\text{H}_2\text{O} \rightarrow \text{H}_2 + \text{O}$]¹⁰⁻¹³. The hydrogen undergoes a hydrogen evolution reaction(HER), as shown in equation 1, and generates gaseous hydrogen^{14,15}. The oxygen undergoes oxygen evolution reaction(OER)(equation 2), which is needed for energy conversion and energy storage¹⁶. Therefore, searching for an ideal material for the photocatalyst is vital for effective photocatalytic water splitting as an alternative energy source.



In 1972, Fujishima and Honda used TiO_2 as a photocatalyst in semiconductor electrochemical photolysis for the first time¹⁷, which paved the way for future research on semiconductor photocatalysis. Thirty years later, researchers started investigating the use of cocatalysts and sacrificial reagents to improve photocatalytic abilities^{18,19}. Now, a variety of different materials and methods have been explored to find an ideal band gap ranging from heterostructures²⁰, to metal and non-metal doping²¹, then to nanostructures²².

Recently, 2D materials have gained attention as their photocatalytic abilities have shown promising results. In particular, several 2D materials have been investigated for photocatalytic water splitting such as SbP_3 ²³, SIn_2Te ²⁴, GaS ²⁵, and MgPSe_3 ²⁵. Monolayers show superior photocatalysis compared to bulk materials due to their maximized surface area, low electron-hole recombination rate, and broad adsorption range^{26–28}. 2D materials have a large surface area available for photocatalytic reactions because they optimize the amount of surface area for a material. They also reduce the probability of electron-hole recombination because the distance that the photogenerated electrons and holes have to travel in order to reach the solid/water interface is reduced^{27,28}. Several recent studies proved the advantages of 2D materials. For example, Zhang et al. recently studied the photocatalytic properties of bulk $\text{Cu}_2\text{ZnSnS}_4$ and monolayer $\text{Cu}_2\text{ZnSnS}_4$. They reported that the monolayer’s band edge positions were narrower to the ideal placement and its overpotentials were lower for the two reactions than the bulk²⁹. In addition, Garg et al. compared the photocatalytic properties of monolayer and bulk CuCl . They demonstrated that the stability of the 2D material was superior to that of the 3D material due to its favorable band edge alignments and its driving force, which compensated the reaction overpotential for OER³⁰. Due to the desirable properties of 2D materials, researchers have investigated a variety of different 2D materials for photocatalysis^{29,31–35}.

In particular, one group of 2D materials, Transition Metal Dichalcogenides (TMDs), have received special attention for their potential as catalysts. TMDs are semiconductors in the form of MX_2 , where M is a transition metal element from group IV (Ti, Zr, or Hf), group V (V, Nb, Ta) or group VI (Mo or W); and X is a chalcogen (S, Se or Te)³⁶. TMDs have high reactivity, reasonable stability, and a suitable band gap^{37,38}. The wettability of TMDs has also been reported in literature. For example, Chhowalla et al. and others have shown 2D TMDs to be chemically stable in aqueous solutions, accessible in experiments, nontoxic, and inexpensive^{39–45}.

Among the numerous TMDs that have been studied, MoS_2 has gained the most popularity due to its adaptable characteristics. It has been doped with many different materials^{36,37,46,47}, combined into heterostructures^{48,49}, and used as a cocatalyst⁵⁰. However, regarding the most important property of a photocatalyst —band gap— Mo_2 is still not ideal. The band gap of Mo_2 is 1.8eV ⁵¹, which is still considerably larger than the ideal

1.23eV band gap.

In order to further narrow the band gap, in this paper, we studied a new TMD material, WSe₂, as a potential photocatalyst. WSe₂ has a similar structure and components to MoS₂, and is currently used in heterostructures. To our knowledge, this is the first time WSe₂ is studied as a potential photocatalyst. We aim to determine the photocatalytic abilities of WSe₂, and whether it can be improved with Cr, Mo, Ta, and Re substitutional doping using first principles calculations.

II. METHOD

The ABINIT simulation package was used to calculate the band structure, Projected Density of States(PDOS), formation energy, and adsorption energy of pristine WSe₂ and Cr, Mo, Ta, and Re doped WSe₂.

A. Computational Methods

Our calculations were based on Density Functional Theory(DFT) in conjunction with the generalized gradient approximations(GGA) for an exchange-correlation functional, as described by Perdew-Burke-Ernzerhof(PBE)⁵². Projector augmented wave(PAW) pseudopotentials were generated with the AtomPAW code⁵³. The electronic configurations and radius cut offs for generating the PAW pseudopotentials are shown in Table I.

TABLE I: The electronic configurations and radius cut offs used to generate the PAW pseudopotentials

Element	Electronic Configuration	Radius cut off(a.u.)
Chromium	[Ne] 3s ² 3p ⁶ 4s ¹ 3d ⁵	2.1
Selenium	[Ar 3d ¹⁰] 4s ² 4p ⁴	2.2
Molybdenum	[Ar 3d ¹⁰] 4s ² 4p ⁶ 5s ¹ 4d ⁵	2.2
Tantalum	[Kr 4d ¹⁰ 4f ¹⁴] 5s ² 5p ⁶ 6s ² 5d ³	2.41
Tungsten	[Kr 4d ¹⁰ 4f ¹⁴] 5s ² 5p ⁶ 6s ² 5d ⁴	2.41
Rhenium	[Kr 4d ¹⁰ 4f ¹⁴] 5s ² 5p ⁶ 6s ² 5d ⁵	2.4

For all materials, the kinetic energy cut off and Monkhorst-Pack k-point grids converged. The self-consistent field(SCF) iterations terminated when the difference between the current and the previous total energy was smaller than 1.0×10^{-10} Hartree twice in a row. The kinetic energy cut off and Monkhorst-Pack kpoint grid values were considered converged when the difference between the current and previous total energy values for all the different data sets were less than 0.0001 Hartree(about 3meV) twice in succession. All of the atomic positions were relaxed before the convergence, and the lattice parameters were relaxed before and after convergence. We applied the Broyden-Fletcher-Goldfarb-Shanno(BFGS) minimization with a maximal force tolerance of 5.0×10^{-5} Hartree/Bohr. Once the maximal force tolerance was reached, the structural relaxation iterations terminated. When the difference between the current and previous total force for all atoms reached 5.0×10^{-6} Hartree/Bohr twice consecutively, the SCF cycle was completed. These relaxed and converged values were then used for total energy calculations.

B. Electronic Structure

We calculated and plotted the band structure of WSe₂ before and after doping using all of the converged values. The high symmetry k-points utilized was $\Gamma(0, 0, 0)$, $K(1/3, 2/3, 0)$, and $M(1/2, 0, 0)$ along the hexagonal Brillouin zone as shown in Figure 1.

We calculated the PDOS for pristine WSe₂ and transition metal doped WSe₂. We plotted the 5d orbital of Tungsten, 4p orbital of Selenium, and the d orbital for the dopants to determine whether the localized states above the Fermi level were filled and whether there was strong hybridization. The Fermi level was set to zero.

C. Energy

In order to calculate the formation energy, we calculated the total energy of WSe₂ before and after doping. The following formula was used to calculate the formation energy:

$$E_{Formation} = E_{total} - E_{WSe_2} - E_{Dopant} + E_W \quad (3)$$

where $E_{Formation}$, E_{total} , E_{WSe_2} , E_{Dopant} , and E_W represent the formation energy, total energy

of doped WSe₂, total energy of pristine WSe₂, total energy of the dopant, and total energy of a Tungsten atom, respectively.

The adsorption energy was calculated in order to determine the interaction strength between the water molecules and the monolayer by calculating the total energy of WSe₂ before and after adsorption of H₂O. The following formula was used to calculate the adsorption energy:

$$E_{Adsorption} = E_{total} - E_{Monolayer} - E_{H_2O} \quad (4)$$

where $E_{Adsorption}$, E_{total} , $E_{Monolayer}$, and E_{H_2O} represent the adsorption energy, total energy of H₂O adsorbed on the WSe₂ surface, total energy of pristine or doped WSe₂ monolayer, and total energy of H₂O, respectively.

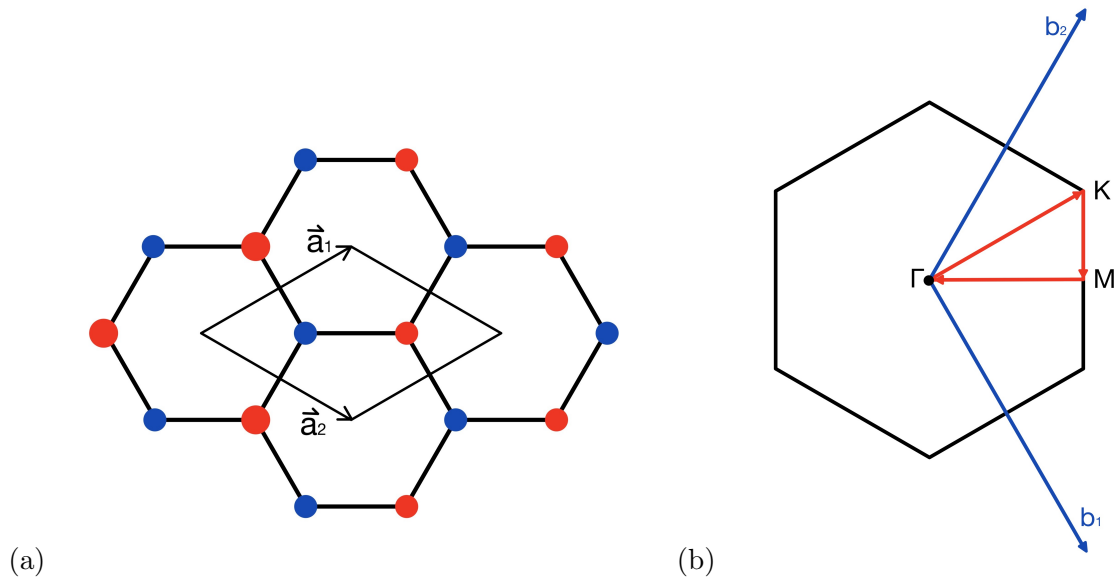


FIG. 1: (a)Primitive cell and(b)First Brillouin Zone of hexagonal lattice with high symmetry k-points

III. RESULTS

We first analyzed the electronic calculations of pristine WSe₂, which were conducted using relaxed and converged values. Next, we demonstrated the effects of Cr, Mo, Ta, and Re doping on WSe₂. The band structure and PDOS of the doped monolayer to those of

the pristine WSe₂ were compared. Finally, we evaluated the formation energy and water adsorption for each monolayer.

A. Criteria for Water Splitting

In order for a material to be a photocatalyst, it must satisfy several band gap requirements. The valence band maximum(VBM) must be more negative than the reduction potential of H⁺/H₂(0eV)^{54,55}. The conduction band minimum(CBM) must be larger than the oxidation potential of O₂/H₂O(1.23eV)^{54,55}. Therefore, the band gap must be larger than 1.23eV. On the other hand, in order for a photocatalyst to efficiently harvest solar energy, the band gap must be smaller than 3.0eV^{6,11}.

B. Photocatalytic Properties of pristine WSe₂

In this paper, we used the hexagonal monolayer structure of WSe₂, which is in the P63/mmc space group. As shown in Figure 2, the structure consists of sandwich layers Se-W-Se, where the Tungsten layer is enclosed with Selenium. The lattice constant for pristine WSe₂ is 6.279 Bohr. The bond length between the Selenium and Tungsten is 4.819 Bohr, and the Se-W-Se bond angle is 82.4°, as listed in Table I. The converged kinetic energy cut off value of WSe₂ is 23 Hartree. The k-points of 4×4×1 and converged kpoint grid 6×6×1 automatically generated by the Monkhorst-Pack scheme were used for structural optimization and self-consistent calculations, respectively. These values were used to conduct the electronic calculations of WSe₂.

As shown in Figure 2(c), WSe₂ has a direct band gap which is slightly higher than 1.5eV. This meets the requirement of a band gap between 1.23eV and 3.0eV. In addition, the band edge positions straddle both the oxidation potential of O₂/H₂O and the reduction potential of H⁺/H₂. These properties establish WSe₂ as a photocatalyst. The PDOS shown in Figure 2(d) indicates that there were no unfilled localized states above the Fermi level. It also shows that the valence band was composed of both the Se 4p and W 5d orbitals, whereas the conduction band was composed mainly of the Se 4p orbital.

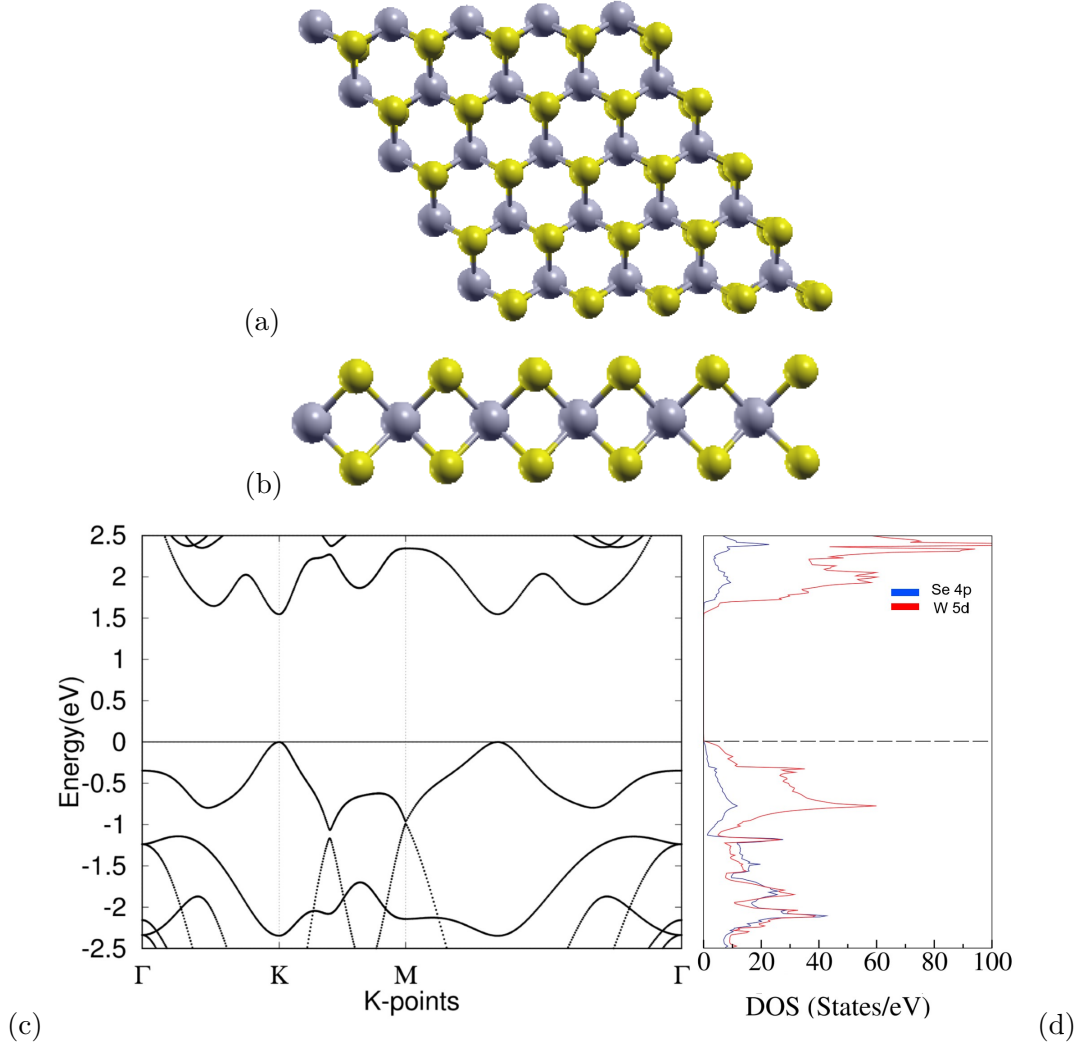


FIG. 2: (a)Top and(b)side view of the pristine WSe₂ monolayer. Purple represents the W atoms, and yellow represent the Se atoms.(c)Band Structure and(d)PDOS of pristine WSe₂. Blue represents Se 4p orbital, and red represents W 5d orbital. The Fermi level is set to 0, which is symbolized as the dotted line.

C. Doping Effect on Band Structure and PDOS

For the doped monolayers, a $3 \times 3 \times 1$ supercell was relaxed and utilized for calculations. We doped the monolayer using substitutional doping, where the center tungsten atom was replaced with the dopant. A $2 \times 2 \times 1$ kpoint grid and the same kinetic energy cut off were used during the calculations.

As shown in Figure 3(a) and Figure 4(a), the Cr doping negatively impacted the

band edge alignments. The Cr dopant caused the shifting of the CBM, as it was the main contributor of the conduction band between 1.1eV and 1.4eV. The new band gap was still direct, however, it was around 1.1eV. The VBM was still at 0, and the CBM was at around 1.1eV, as previously stated, due to the Cr dopant. This is below the oxidation potential of O_2/H_2O (1.23eV), therefore, Cr doped WSe_2 does not meet the criteria to be a photocatalyst.

In Figure 3(b) and Figure 4(b), it is observed that the Mo doping did not change the band gap alignments. The VBM and CBM shifted from the K point to the Γ point, however, the band gap was still direct and around 1.5eV, with the VBM at 0eV and the CBM at around 1.5eV, which was very similar to pristine WSe_2 . Also shown in Figure 4(b) is the hybridization between the Mo 4d and W 5d orbitals through their simultaneous peaks and troughs, especially between -1 and 0eV. This fits the criteria for Mo doped WSe_2 to be a photocatalyst, however, it does not increase the number of photons adsorbed because the band gap has not decreased.

The Ta doping improved the band edge alignments, as shown in Figure 3(c) and Figure 4(c). Similar to the Mo doped WSe_2 , both the VBM and CBM shifted to the Γ point, thus maintaining the direct band gap. The CBM was lowered by about 0.2eV, and the VBM lowered by about 0.1eV, thus making the new band gap around 1.4eV. Compared to the others, Ta doped WSe_2 had the smallest band gap without going below 1.23eV. Furthermore, the CBM and VBM straddled the oxidation potential of O_2/H_2 and the reduction potential of H^+/H_2 . It was also observed in Figure 4(c) that there were no unfilled localized states above the Fermi level and some hybridization between the Ta 5d orbital and the W 5d orbital. However, the hybridization was not as strong as that of the Mo 4d orbital and the W 5d orbital shown in Figure 4(b). Therefore, with the ideal band edge positions and hybridization, Ta doped WSe_2 is a promising photocatalyst.

As shown in Figure 3(d) and Figure 4(d) the Re doping hindered the band edge alignments. The VBM shifted to about -1.6eV, and the CBM shifted to about -0.4eV. Therefore, the band gap is smaller than 1.23eV, and the band edge positions do not qualify Re doped WSe_2 to be a photocatalyst.

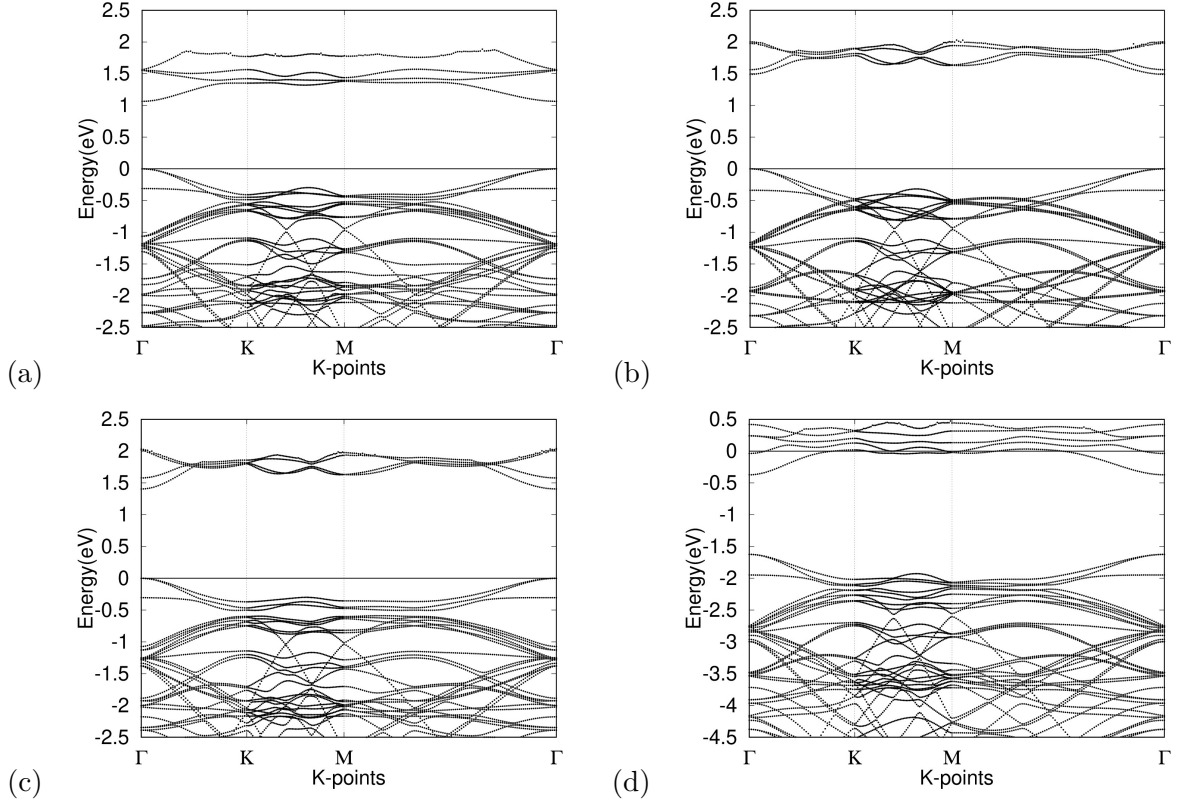


FIG. 3: Band structure for (a)Cr, (b)Mo, (c)Ta, and (d)Re doped WSe_2

D. Formation Energy

The formation energy determines how facile it is to perform substitutional doping and how stable the doped monolayer is. If the formation energy is negative, it indicates that the formation is an exothermic process. The more negative the formation energy is, the more facile the doping process is and the more stable the monolayer is.

As shown in Table II, the formation energies for Mo(-0.448eV) and Ta(-0.922eV) doped WSe_2 were negative, indicating that they underwent an exothermic process, whereas Cr(0.387eV) and Re(0.845eV) doped WSe_2 underwent an endothermic process. The formation energies were relatively small, however, out of the 4 different doped monolayers, the Ta doped WSe_2 monolayer was the most energetically favorable.

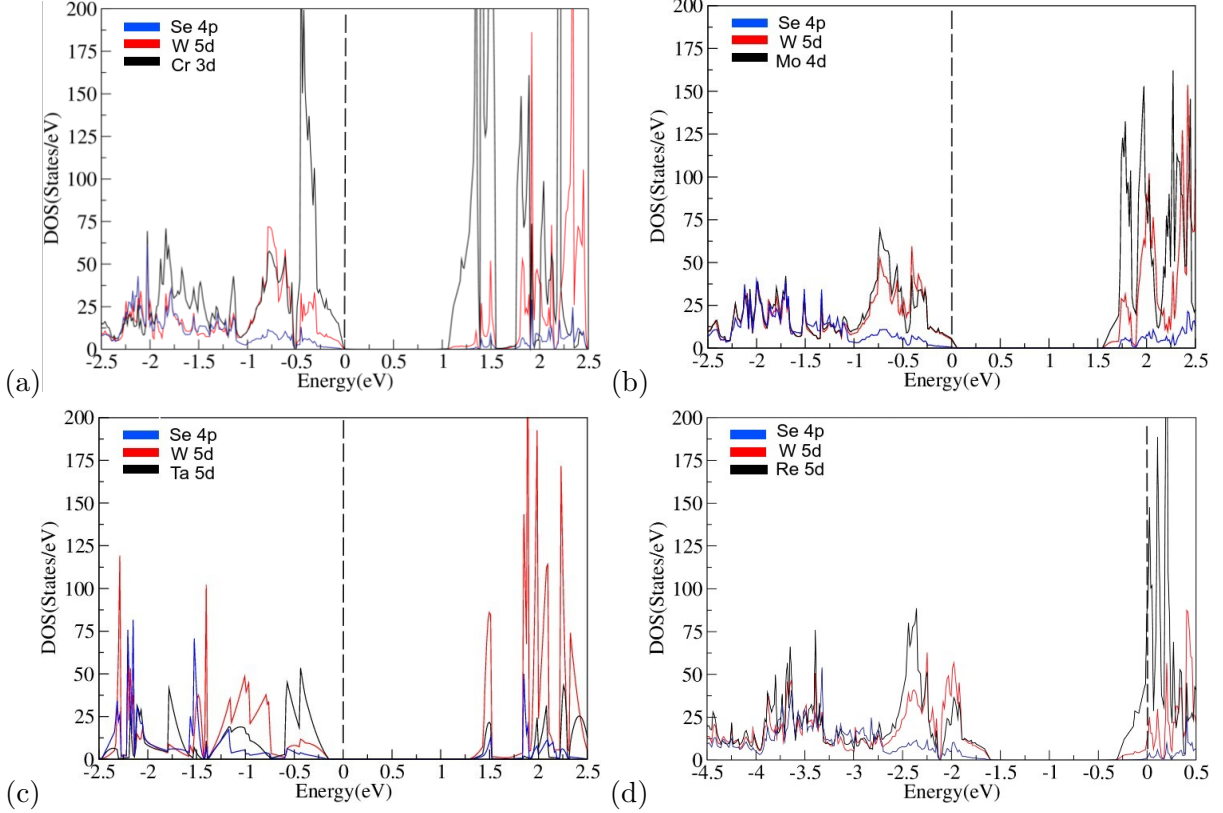


FIG. 4: PDOS for (a)Cr, (b)Mo, (c)Ta, and (d)Re doped WSe_2 . Blue, red, and black represent Se 4p, W 5d, and the dopant's d orbital, respectively. The dotted line symbolizes the Fermi level, which is set to 0.

E. Water Adsorption

The water molecule was placed in the hollow site above the dopant because Peng et al. determined that it was the most stable adsorption configuration⁵⁶. A negative adsorption energy means that the water molecule can be adsorbed energetically favorably. The more negative the adsorption energy is, the stronger the interaction is between the water molecules and the monolayer.

The water adsorption for each monolayer is listed in the table II. For pristine WSe_2 , the adsorption energy was -0.1184eV , which is relatively weak. This was not improved by the dopants. For the Mo doped WSe_2 monolayer, the adsorption energy was -0.1174eV , and for the Ta doped WSe_2 monolayer, surprisingly, the adsorption energy was -0.0439eV . The pristine WSe_2 and Mo doped WSe_2 adsorption values were not as negative as we expected, how-

ever, they were more negative than the Ta doped WSe₂ monolayer. This suggests stronger interactions between the water molecules and the pristine and Mo doped WSe₂ monolayers. Despite the weaker interactions, the adsorption energy values were negative for all three monolayers, meaning that the water molecules can be adsorbed energetically favorably.

TABLE II: Bond angles(Se-W-Se), bond lengths(Se-W), Formation energy of transition metal(E_f), and Adsorption energy of water(E_a) for pristine and Cr, Mo, Ta, Re doped WSe₂

Configuration	Bond Angle(°)	Bond Length(Bohr)	E_f (eV)	E_a (eV)
WSe ₂	82.4	4.819	-	-0.1184
WSe ₂ (Cr)	82.8	4.819	0.387	-
WSe ₂ (Mo)	82.3	4.819	-0.448	-0.1174
WSe ₂ (Ta)	81.9	4.819	-0.922	-0.0439
WSe ₂ (Re)	82.5	4.819	0.845	-

IV. DISCUSSION

Photocatalytic water splitting is a promising renewable energy source as an alternative for limited fossil fuels. The effectiveness of the conversion from solar energy to hydrogen fuel relies primarily on the material. Previously, researchers studied different TMDs such as WS₂³⁵, MoS₂^{36,37,46,51,57}, and PdSe₂⁵⁸. These materials perform well in many properties such as strong adsorption stability(WS₂) and promising abilities for HER, however, their band gaps are still not ideal. In this paper, we aim to improve upon this band gap by studying a new TMD material, WSe₂.

Currently, WSe₂ is used in heterostructure photocatalysts. To our knowledge, this is the first time that pristine monolayer WSe₂ and doped WSe₂ have been studied as potential photocatalysts. In particular, our calculations show excellent band gaps and band edge positions, the two most important properties of a photocatalyst. For band gaps, our calculations are 1.5eV for pristine WSe₂, 1.5eV for Mo doped WSe₂, and 1.4eV for Ta doped WSe₂, which are closer to 1.23eV(the ideal band gap which most efficiently harvest solar energy^{6,11}) than previous studies. For example, Long et al(2018) reported a band gap of 2.28eV for PdSe₂⁵⁸, Ryou et al(2016) reported 1.8eV for MoS₂⁵¹, and Yao et al(2019) reported 2.36eV for SbP₃

and 1.45eV for GaP³²³.

Furthermore, our calculations demonstrated that the band edge positions of pristine, Mo doped, and Ta doped WSe₂ are an improvement over those of previously reported materials. It is well known that for an ideal photocatalyst, the VBM is the reduction potential of H⁺/H₂, i.e., 0eV; and the CBM is the oxidation potential of O₂/H₂O, i.e., 1.23eV. Previously, Zhang et al reported approximately -0.3eV as the VBM of MoS₂ and around 2eV as the CBM⁵⁷. In Bui et al's 2015 paper, the VBM for WS₂ was around -0.2eV and the CBM was about 1.7eV³⁵. In our paper, for two materials, pristine and Mo doped WSe₂, the VBM is 0eV and the CBM is 1.52eV. For the third material, Ta doped WSe₂, the VBM is -0.1eV and the CBM is 1.32eV. For all three materials, the VBM and CBM are much closer to the ideal band edge positions of 0eV and 1.23eV than the previous papers, suggesting a more efficient collection of solar energy.

In addition, as previously discussed, the formation energies for two studied materials, Mo and Ta doped WSe₂, are negative, indicating a desired exothermic process with stable doped monolayers. Between the Mo doped WSe₂ and the Ta doped WSe₂, the Ta doped WSe₂ monolayer is the most stable. On the other hand, the formation energies for the Cr and Re doped WSe₂ are positive, suggesting an unstable monolayer. Hence, Cr and Re doped WSe₂ were dropped in the calculations.

Despite all the desired properties, one limitation of pristine and doped WSe₂ is that their performance is less satisfactory for water adsorption. The adsorption energies for pristine WSe₂, Mo doped WSe₂, and Ta doped WSe₂ are -0.1184, -0.1174, and -0.0439 respectively, indicating stable but weak water adsorption.

Some of the future works can consider calculating spin-orbital coupling, predicting the reaction barrier, and using alternative methods such as the Heyd–Scuseria–Ernzerhof(HSE) exchange–correlation functional and GW approximation(GWA) to calculate the electronic structures, which can then be compared to the PBE exchange–correlation functional method.

V. CONCLUSION

Aiming to improve the band gap of previously reported photocatalytic materials, we studied a new TMD material, WSe₂, as a monolayer. To our knowledge, this is the first

report of using transition metal doped WSe₂ as potential photocatalysts for photocatalytic water splitting. We used first principles calculations to evaluate the photocatalytic abilities of pristine WSe₂ as well as Cr, Mo, Ta, and Re doped WSe₂. Our calculations showed that the band gaps and band edge positions of three of our studied materials (pristine, Mo doped, and Ta doped WSe₂) are ideal for water splitting. Compared to previous studies of similar materials, our materials demonstrate more desirable band gaps: 1.5eV for pristine WSe₂ and Mo doped WSe₂, and 1.4eV for Ta doped WSe₂, which are closer to the ideal 1.23eV; The band edge positions of our materials are also closer to the reduction potential of H⁺/H₂ and the oxidation potential of O₂/H₂O. In addition, Mo and Ta doped WSe₂ monolayers undergo an exothermic process, indicating stable monolayers. Of the three selected materials, pristine WSe₂ exhibits the strongest water adsorption abilities. Our results substantiates pristine, Mo doped, and Cr doped WSe₂ as potential photocatalysts for water splitting.

VI. ACKNOWLEDGEMENTS

The authors would like to acknowledge Dr. Gefei Qian for his technical support.

VII. AUTHOR DECLARATIONS

The authors have no conflicts to disclose.

-
- ¹ U.S. Energy Information Administration. History of energy consumption in the united states, 1775–2009, 2011.
- ² U.S. Energy Information Administration. In 2018, the united states consumed more energy than ever before, 2019.
- ³ Drew DeSilver. Renewable energy explained, 2020.
- ⁴ U.S. Energy Information Administration. Renewable energy is growing fast in the u.s., but fossil fuels still dominate, 2020.
- ⁵ Gioietta Kuo. When fossil fuels run out, what then?, 2019.
- ⁶ Yilimiranmu Rouzhahong, Mariyemu Wushuer, Mamatrishat Mamat, Qing Wang, and Qian Wang. First principles calculation for photocatalytic activity of gaas monolayer. *Scientific Reports*, 10, 2020.
- ⁷ Ramazan Asmatulu and Waseem S. Khan. *Synthesis and Applications of Electrospun Nanofibers*. Elsevier, 2019.
- ⁸ Steven Suib. *New and Future Developments in Catalysis*. Elsevier, 2013.
- ⁹ Jeffrey M. Lipshultz and David W. C. MacMillan. *The Strem Chemiker*. Strem Chemicals, Inc., 2018.
- ¹⁰ Shanshan Chen, Tsuyoshi Takata, and Kazunari Domen. Particulate photocatalysts for overall water splitting. *Nature Reviews Materials*, 2017.
- ¹¹ P.A. Ash and K.A. Vincent. *Encyclopedia of Interfacial Chemistry*. Elsevier, 2018.
- ¹² Phuc D. Nguyen, Tuan M. Duong, and Phong D. Tran. Current progress and challenges in engineering viable artificial leaf for solar water splitting. *Journal of Science: Advanced Materials and Devices*, 2:399–417, 2017.
- ¹³ Kazuhiro Takanabe. Photocatalytic water splitting: Quantitative approaches toward photocatalyst by design. *Journal of Science: Advanced Materials and Devices*, 7:8006–8022, 2017.
- ¹⁴ K. Kakaei, M. D. Esrafil, and A. Ehsani. *Graphene Surfaces*. Academic Press, 2019.
- ¹⁵ U.S. Department of Energy’s Office of Energy Efficiency and Renewable Energy’s. Hydrogen production and distribution.
- ¹⁶ Zhixiong Cai, Qihong Yao, and Xiaoru Wang. Novel nanomaterials for biomedical, environ-

- mental and energy applications. *Micro and Nano Technologies*, pages 435–464, 2019.
- ¹⁷ A. Fujishima and K. Honda. Electrochemical photolysis of water at a semiconductor electrode. *Nature*, 238:37–38, 1972.
- ¹⁸ Iwase Akihide, Kato Hideki, and Kudo Akihiko. A novel photodeposition method in the presence of nitrate ions for loading of an iridium oxide cocatalyst for water splitting. *Chemistry Letters*, 34:946–947, 2005.
- ¹⁹ Anna Galińska and Jerzy Walendziewski. *Energy Fuels*. American Chemical Society, 2005.
- ²⁰ Sake Wang, Chongdan Ren, Hongyu Tian, Jin Yu, and Minglei Sun. Mos₂/zno van der waals heterostructure as a high-efficiency water splitting photocatalyst: a first-principles study. *Phys. Chem. Chem. Phys.*, 20:13394–13399, 2018.
- ²¹ Min Li, Jingfa Li, Cong Guo, and Lei Zhang. Doping bismuth oxyhalides with indium: A dft calculations on tuning electronic and optical properties. *Chemical Physics Letters*, 705:31–37, 2018.
- ²² S. Kment, K. Sivula, A. Naldoni, S.P. Sarmah, H. Kmentova, M. Kulkarni, Y. Rambabu, P. Schmuki, and R. Zboril. Feo-based nanostructures and nanohybrids for photoelectrochemical water splitting. *Progress in Materials Science*, 110, 2020.
- ²³ Sai Yao, Xu Zhang, Zihe Zhang, An Chen, and Zhen Zhou. 2d triphosphides: Sbp₃ and gap₃ monolayer as promising photocatalysts for water splitting. *International Journal of Hydrogen Energy*, 44, 2019.
- ²⁴ Yujie Baia, Qinfang Zhanga, Ning Xua, Kaiming Dengb, and Erjun Kan. The janus structures of group-iii chalcogenide monolayers as promising t photocatalysts for water splitting. *Applied Surface Science*, 478, 2019.
- ²⁵ Arunima K. Singh, Kiran Mathew, Houlong L. Zhuang, and Richard G. Hennig. Computational screening of 2d materials for photocatalysis. *J. Phys. Chem. Lett.*, 6, 2015.
- ²⁶ Chen Long, Yan Liang, Hao Jin, Baibiao Huang, and Ying Dai. Pdse₂: Flexible two-dimensional transition metal dichalcogenides monolayer for water splitting photocatalyst with extremely low recombination rate. *ACS Appl. Energy Mater*, 2018.
- ²⁷ Y. Li, C. Gao, R. Long, and Y. Xiong. Photocatalyst design based on two-dimensional materials. *Materials Today Chemistry*, 11, 2019.
- ²⁸ Shengyao Wu, Yanqing Shen, Xu Gao, Yanyan Maa, and Zhongxiang Zhou. The novel two-

- dimensional photocatalyst SnS_3 with enhanced visible-light absorption for overall water splitting. *Nanoscale*, 40, 2019.
- ²⁹ Ruifen Zhang, Xin Wen, Fen Xu, Qiubo Zhang, and Lixian Sun. A density functional theory study of the $\text{Cu}_2\text{ZnSnS}_4$ monolayer as a photo-electrointegrated catalyst for water splitting and hydrogen evolution. *J. Phys. Chem. C*, 124, 2020.
- ³⁰ Priyanka Garg, Kuber Singh Rawat, Gargee Bhattacharyya, Sourabh Kumar, and Biswarup Pathak. Hexagonal CuCl monolayer for water splitting: A dft study. *ACS Appl. Nano Mater.*, 2, 2019.
- ³¹ Man Qiao, Jie Liu, Yu Wang, Yafei Li, and Zhongfang Chen. PdSeO_3 monolayer: Promising inorganic 2d photocatalyst for direct overall water splitting without using sacrificial reagents and cocatalysts. *J. Am. Chem. Soc.*, 140, 2018.
- ³² Junkang Xu, Qiang Wan, Masakazu Anpo, and Sen Lin. Bandgap opening of graphdiyne monolayer via b, n-codoping for photocatalytic overall water splitting: Design strategy from dft studies. *J. Phys. Chem. C*, 124, 2020.
- ³³ M. R. Ashwin Kishore and Ponniah Ravindran. Tailoring the electronic band gap and band edge positions in the C_2N monolayer by p and as substitution for photocatalytic water splitting. *J. Phys. Chem. C*, 121, 2017.
- ³⁴ Huanhuan Li, Yong Wu, Lei Li, Yinyan Gong, Lengyuan Niu, Xinjuan Liu, Tao Wang, Changqing Sun, and Can Li. Adjustable photocatalytic ability of monolayer g- C_3N_4 utilizing single-metal atom: Density functional theory. *Applied Surface Science*, 457, 2018.
- ³⁵ Viet Q Bui, Tan-Tien Pham, Duy A Le, Cao Minh Thi, and Hung M Le. A first-principles investigation of various gas (CO , H_2O , NO , and O_2) absorptions on a WS_2 monolayer: stability and electronic properties. *Journal of Physics: Condensed Matter*, 27, 2015.
- ³⁶ Hui Pan. Metal dichalcogenides monolayers: Novel catalysts for electrochemical hydrogen production. *Scientific Reports*, 2, 2014.
- ³⁷ Satvik Lolla and Xuan Luo. Tuning the catalytic properties of monolayer MoS_2 through doping and sulfur vacancies. *Applied Surface Science*, 507, 2020.
- ³⁸ Lin Ju, Mei Bie, Jing Shang, Xiao Tang, and Liangzhi Kou. Janus transition metal dichalcogenides: a superior platform for photocatalytic water splitting. *JPhys Materials*, 2020.
- ³⁹ Chhowalla Manish, Hyeon Suk Shin, Goki Eda, Lain-Jong Li, Kian Ping Loh, and Hua Zhang.

- The chemistry of two-dimensional layered transition metal dichalcogenide nanosheets. *Nature Chemistry*, 5, 2013.
- ⁴⁰ Hai Li, Jumiati Wu, Zongyou Yin, and Hua Zhang. Preparation and applications of mechanically exfoliated single-layer and multilayer mos2 and wse2 nanosheets. *Nature Chemistry*, 47:1067–1075, 2014.
- ⁴¹ Chuang Wang, Xiao-Dong Zhu, Ke-Xin Wang, Liang-Liang Gu, Sheng-You Qiu, Xiao-Tian Gao, Peng-Jian Zuo, and Nai-Qing Zhang. A general way to fabricate transition metal dichalcogenide/oxide-sandwiched mxene nanosheets as flexible film anodes for high-performance lithium storage. 2019.
- ⁴² Chenxi Zhang, Jun Lou, and Jizhou Song. A cohesive law for interfaces in graphene/hexagonal boron nitride heterostructure. *Journal of Applied Physics*, 115, 2014.
- ⁴³ Xing Zhou, Lin Gan, Wenming Tian, Qi Zhang, Shengye Jin, Huiqiao Li, Yoshio Bando, Dmitri Golberg, and Tianyou Zhai. Ultrathin snse2 flakes grown by chemical vapor deposition for high-performance photodetectors. *Advanced Materials*, 27:8035–8041, 2015.
- ⁴⁴ Xuming Wu, Lun Xiong, Yulin Feng, Cong Wang, and Guoying Gao. The half-metallicity and the spin filtering, ndr and spin seebeck effects in 2d ag-doped snse2 monolayer. *Advanced Materials*, 150, 2019.
- ⁴⁵ Yingcai Fanab, Junru Wang, and Mingwen Zhao. Spontaneous full photocatalytic water splitting on 2d mose2/snse2 and wse2/snse2 vdW heterostructures. *Nanoscale*, 2019.
- ⁴⁶ Guang-Zhao Wang, Hong-Kuan Yuan, An-Long Kuang, and Hong Chen. Anion–anion co-doped monolayer mos2 for visible light photocatalysis. *Phys. Status Solidi B*, 2017.
- ⁴⁷ Kuilin Lv, Weiqun Suo, Mingda Shao, Ying Zhu, Xingpu Wang, Jingjing Feng, Mingwei Fang, and Ying Zhu. Nitrogen doped mos2 and nitrogen doped carbon dots composite catalyst for electroreduction co2 to co with high faradaic efficiency. *ACS Appl. Energy Mater*, 16, 2019.
- ⁴⁸ Bin Gao, Jin-Rong Zhang, Lang Chen, Junkang Guo, Sheng Shen, Chak-Tong Au, Shuang-Feng Yin, and Meng-Qiu Cai. Density functional theory calculation on two-dimensional mos2/biox (x=cl, br, i) van der waals heterostructures for photocatalytic action. *Applied Surface Science*, 492, 2019.
- ⁴⁹ Xuwen Xu, Xiaoli Ge, Xin Liu, Lanlan Lia, Kun Fub, Yao Dong, Fanbin Meng, Ruihao Si, and Minghui Zhang. Two-dimensional m2co2/mos2 (m = ti, zr and hf) van der waals heterostruc-

- tures for overall water splitting: A density functional theory study. *Ceramics International*, 46, 2020.
- ⁵⁰ Mengmeng Shao, Yangfan Shao, Shengjie Ding, Rui Tong, Xiongwei Zhong, Lingmin Yao, Weng Fai Ip, Baomin Xu, Xing-Qiang Shi, Yi-Yang Sun, Xuesen Wang, and Hui Pan. Carbonized mos₂: Super-active co-catalyst for highly efficient water splitting on cds. *ACS Sustainable Chem. Eng.*, 7, 2019.
- ⁵¹ Effat Sitara, Habib Fahad Ehsan, Muhammad and Nasir, Sadia Iram, and Syeda Aqsa Batoool Bukhari. Synthesis, characterization and photocatalytic activity of mos₂/znse heterostructures for the degradation of levofloxacin. *catalysts*, 10, 2020.
- ⁵² Zhonglu Guo, Jian Zhou, Linggang Zhua, and Zhimei Sun. Mxene: a promising photocatalyst for water splitting. *Journal of Materials Chemistry A*, 29, 2016.
- ⁵³ ABINIT. Paw atomic dataset(s) for selenium, 2018.
- ⁵⁴ Ramazan Asmatulu and Waseem S. Khan. *Synthesis and Applications of Electrospun Nanofibers*. Elsevier, 2019.
- ⁵⁵ Fenggong Wang, Cristiana Di Valentin, and Gianfranco Pacchioni. Doping of wo₃ for photocatalytic water splitting: Hints from density functional theory. *J. Phys. Chem. C*, 116, 2012.
- ⁵⁶ Qiong Peng, Rui Xiong, Baisheng Sa, Jian Zhou, Cuilian Wen, Bo Wu, Masakazu Anpoc, and Zhimei Sun. Computational mining of photocatalysts for water splitting hydrogen production: two-dimensional in-se-family monolayers. *Catal. Sci. Technol.*, 7, 2017.
- ⁵⁷ Zheng Zhang, Kai Chen, Qiang Zhao, Mei Huang, and Xiaoping Ouyang. Effects of noble metal doping on hydrogen sensing performances of monolayer mos₂. *Mater. Res. Express*, 7, 2020.
- ⁵⁸ Chen Long, Yan Liang, Hao Jin, Baibiao Huang, and Ying Dai. Pdse₂: Flexible two-dimensional transition metal dichalcogenides monolayer for water splitting photocatalyst with extremely low recombination rate. *ACS Appl. Energy Mater*, 2017.